# Title: Bending Unwinds DNA

**Authors:** Soumya Chandrasekhar[†‡], Thomas P. Swope[†‡], Fatemeh Fadaei[†], Daniel R. Hollis[†], Rachel Bricker[†], Draven Houser[†], John Portman*[†], Thorsten L. Schmidt*[†]

Affiliation: †Department of Physics, Kent State University, Kent, OH, 44242, USA.

‡Contributed equally.

*Corresponding authors. Email: jportman@kent.edu; tschmi21@kent.edu

**Abstract:** In biology, DNA is often tightly bent to small radii. Solely based on the groove asymmetry, a 30-year-old theoretical paper predicted that such bending should unwind DNA, but this effect has not been directly experimentally quantified so far. We developed a ligation-based assay with nicked DNA circles of variable length, thereby decoupling the twist-dependent ligation efficiency from the large bending strain which dominates conventional circularization assays. We demonstrate that tightly bent DNA indeed unwinds to over 11 base pairs/turn, exactly as predicted. Our discovery requires reassessing the molecular mechanisms and energetics of all processes where DNA is tightly bent or relaxed again, including DNA packaging, gene regulation and expression.

**One-Sentence Summary:** When DNA is bent to radii found in nucleosomes and regulatory elements, its helical repeat increases to over 11 base pairs/turn.

## Introduction

In all cells and viruses, DNA is twisted and bent in a highly dynamic way. For example, two meters of human DNA is tightly wrapped around 30 million histone octamers, compacting it into a nucleus measuring mere micrometers across. During gene expression, DNA unbinds from the nucleosome and relaxes its mechanical stress. DNA is also tightly bent in nanometer-sized virus capsids, bacteria, or complexes with many transcription factors that regulate gene expression. An accurate physical model of tightly bent DNA is therefore essential to understand the molecular mechanisms and energetics of many biological processes (*1*, *2*).

The twistable wormlike chain (TWLC) is the standard elastic model for DNA and treats DNA as an inextensible rod with elastic moduli controlling twist and bend deformations (*3*). It accurately predicts the circularization probabilities of long linear DNA fragments (*4–8*). Some studies suggested extreme bendability for short fragments (*9*, *10*), but were criticized for the choice of certain experimental parameters. Moreover, sharp kinks that release bending and torsional stress likely occur during these experiments (**Fig. 1A-B, Supplementary Note 1**). Therefore, tightly bent DNA is still widely considered compatible with the TWLC model (*11–16*).

Twisting and bending deformations are treated as independent by the TWLC model (*3*), but a twist-bend coupling (TBC) was postulated 30 years ago based solely on the asymmetry in the bending moduli of the major and minor grooves by Marko and Siggia (*17*). Their theoretical paper predicted that DNA should significantly unwind when bent into radii that are well below the persistence length (50 nm). However, there is no direct experimental quantification for this consequential prediction.

## Helical repeat $h$ of DNA

B-DNA has an average relaxed helical repeat $h_0$ of 10.45 (±0.05) base pairs (bp) per helical turn, which was determined by topoisomer analysis of long plasmids (*18*), hydroxyl radical digest (*19*) as well as numerous circularization experiments using fragments of a few hundred bp (*4–8*). While DNA is under low bending stress in those experiments, it is often tightly bent in biology. For example, the radius of curvature in the nucleosome is only 4.5 nm – just 10 % of its persistence length, and DNA is considerably overwound at $h = 10.1\ (\pm 0.1)\ bp/turn$ (*19*, *20*). On the other hand, recent all-atom molecular dynamics (MD) simulations of protein-free DNA circles at similar radii predict $h_0 = 11.25\ bp/turn$ (*21–23*).

## Nicked minicircle assay

Here, we present an assay designed to measure $h_0$ and TBC in tightly bent DNA using nicked minicircles of different lengths that consist of one covalently circularized strand and one linear complementary strand (**Fig. 1C**). The nick is the point where the 5' and 3' ends of the linear strand meet and is mechanically the weakest point in the structure. Unlike linear fragments in circularization experiments, this complex can neither unloop nor dimerize, which eliminates the impact of bending stress on the yield of complex formation. Instead, three different states exist for double-stranded circles with a nick: (i) a "stacked" state (**Fig. 1C3**) where the ends of the linear strand are aligned in a conformation that is geometrically indistinguishable from a fully ligated or catenated circle; (ii) a "kinked" or sharply bent state (**Fig. 1C2**) which has a characteristic teardrop shape and can be induced through bending stress; and (iii) a "kinked + twisted" state (**Fig. 1C1**) where the ends are twisted out of alignment. Kinking reduces bending

stress in small circles, as the curvature is lower overall. The transition from a kinked to a stacked state is stabilized by additional $\pi$-stacking between nucleobases but destabilized by increased bending stress; nevertheless, the energy difference between these states is small compared to the energy required for looping a linear duplex of the same length (**Fig 1**A-B). To stack the "kinked + twisted" conformation (**Fig 1**C1), the two ends cannot be realigned through bending alone; an additional twisting energy must be overcome, either by over- or underwinding.

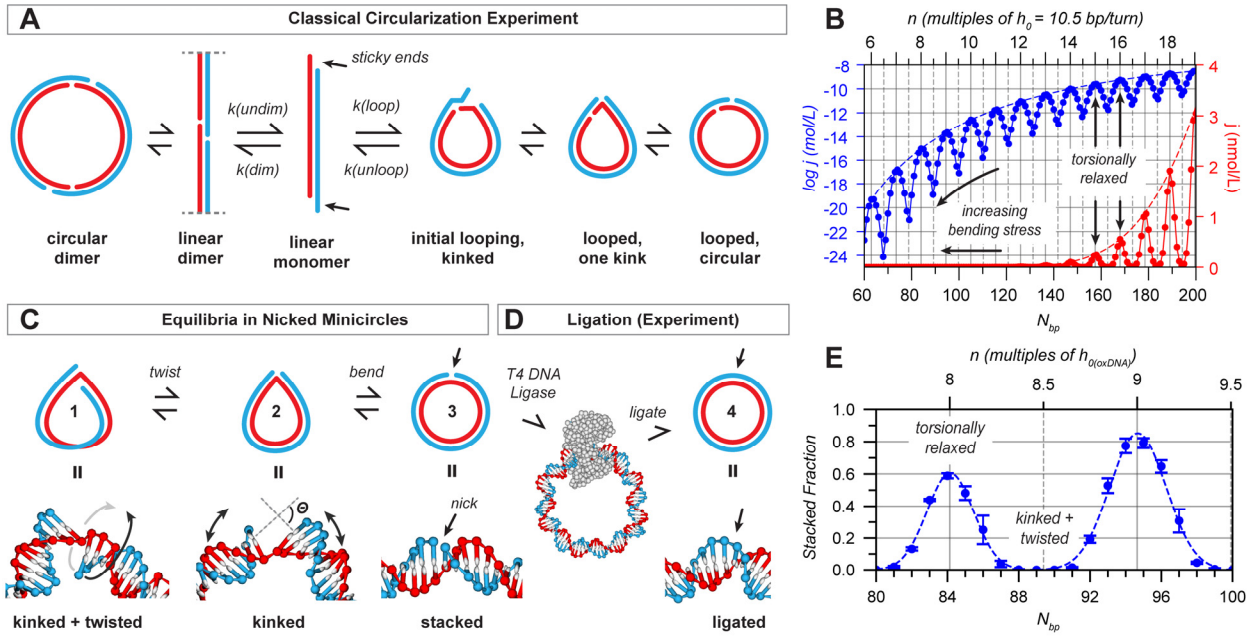


***Fig. 1. A classical circularization experiment (A-B) and states of nicked minicircles (C-E).*** *(**A**) In classical circularization experiments, a linear monomer with self-complementary sticky ends is in equilibrium with a looped and a dimer form. The circular conformation (right) is likely reached through kinked transition states with reduced mechanical stress (*12, 14–16*). (**B**) Plot displaying j-factors, or theoretical circularization probabilities for DNA fragment lengths of* $N_{bp} = 60 - 200\ bp$ *calculated from the Shimada-Yamakawa model (*3*),(**Supplementary Notes 1-2**). Blue: logarithmic scale; Red: linear scale. (**C**) In nicked minicircles (our assay), the ends of the linear strands can adopt three different states: (**1**) kinked + twisted, (**2**) kinked, and (**3**) stacked. See **Fig. S2** for analysis of kink angles* $\theta$*. (**D**) We hypothesize that in a ligation experiment, only the ends of the stacked configuration (**3**) can be joined into a fully ligated circle (**4**). (**E**) Plot of the fraction of stacked configurations from oxDNA simulations of nicked circles between 80-100 bp. Dotted line: Gaussian fits. Note that oxDNA does not show a significant change of the helical repeat for tightly bent DNA and that* $h_0$ *differs between oxDNA and our experiments (see **Fig. 3**, **Fig. 5**). Images in C-D (bottom) are representative snapshots from oxDNA simulations. Illustration of complex with T4 DNA ligase (PDBID: 6DT1) is for size comparison only. All images are rendered with oxView (*24, 25*). Supplementary Movies S1-4 illustrate dynamics and twist angle fluctuation.*

## oxDNA simulations

We first simulated the equilibria between the stacked and kinked states with oxDNA, a computationally inexpensive coarse-grained MD simulation model that reproduces the mechanical properties of canonical B-DNA very well (*26*). Nicked minicircles with a circumference of $N_{\mathrm{bp}} = 80 - 100\ bp$ were simulated and the equilibrium fraction of stacked configurations was determined through a geometrical analysis of the bases around the nick (**Fig. 1C**, Methods and **Fig. S1**). The two maxima in the stacked fractions at $N_{\mathrm{bp}} = 84.1\ bp$ and 94.6 bp indicate ideal contour lengths for minicircles with minimal torsional strain. Maxima are expected to appear at integer multiples of the natural helical repeat, or $N_{bp} \approx nh_0$ for integer $n$. The twist $Tw$ (in helical turns) of the stacked configurations centered about each maximum is $Tw = 8$ and $Tw = 9$, respectively. The ratios of the contour lengths ($N_{bp}$) at the maxima and corresponding twists ($Tw$) then indicate a relaxed helical repeat $h_0 \approx \frac{84.1\ bp}{8\ turn} \approx \frac{94.6\ bp}{9\ turn} \approx 10.52\ bp/turn$ in good agreement with the expected relaxed helical repeat in the oxDNA2 model $h_{0(\mathrm{oxDNA})} = 10.55\ bp/turn$. While twist-bend coupling has been studied in oxDNA2 and results in unique properties like "twist waves" in tightly bent DNA (*27*), the helical repeat of minicircles remains nearly the same as unbent DNA in this model.

Hardly any stacking is observed near the minima, which occur near half-integer multiples of $h_{0(\mathrm{oxDNA})}$ or where $N_{bp} \approx \left(n + \frac{1}{2}\right) h_{0(oxDNA)}$ (**Fig. 1C1**). For these lengths, the minicircles are generally kinked with a most probable kink angle of about 100 degrees (see **Fig. S2**). For $N_{bp} \approx nh_{0(oxDNA)}$, circles are mostly stacked (~60 % and ~80% of simulation snapshots for circles with 8 and 9 helical turns, respectively). Simulating equilibria of a classical looping experiment on the other hand would be impossible with oxDNA as looping is an extremely rare event due to the large free energy cost of circularization of short DNA segments (*14*).

**Ligation experiments**

We next measured the helical repeat of small minicircles through ligation experiments. We hypothesize that only the stacked junctions can be ligated, as only this configuration presents the terminal 5' phosphates and the 3' OH groups close enough for diester bond formation. Maximum ligation yields should therefore be observed when torsional strain is minimal at $N_{bp} \approx nh_0$.

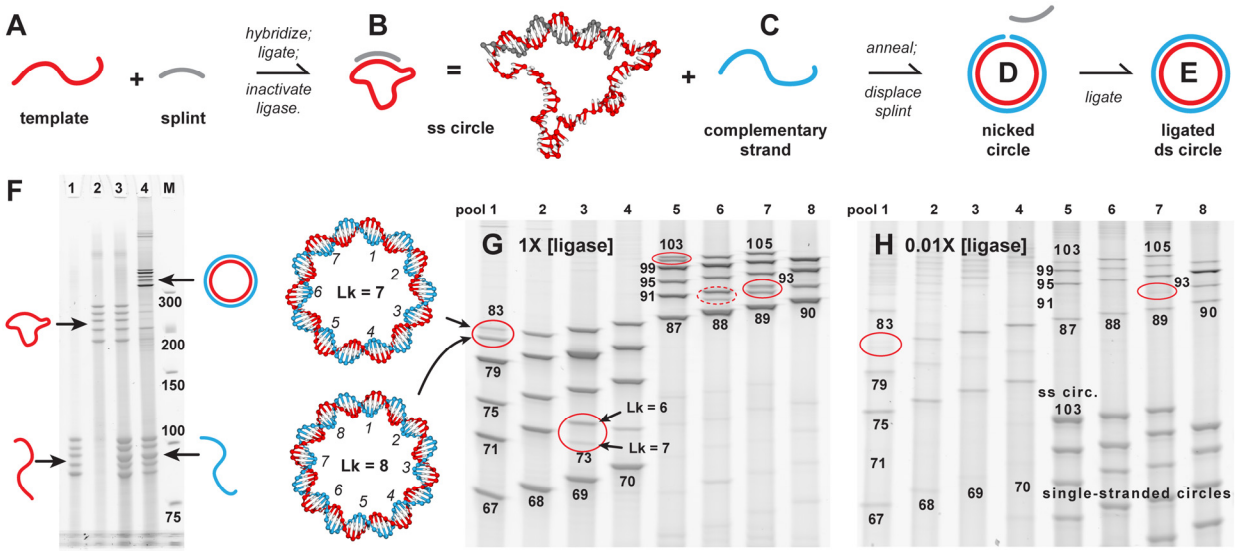


***Fig. 2. Experimental ligation of nicked circles of different lengths.*** *(**A**) Splint ligation of oligonucleotides (67-105 nt) produces ss minicircles (**B**). oxDNA simulation snapshot illustrates flexibility of ss region. (**C**) Respective complementary strands are annealed to yield nicked circles (**D**), which can then be enzymatically ligated into double-stranded circles (**E**). (**F**) Denaturing PAGE gel of (1) 5 oligonucleotides (same as pool 7) before, and (2) after splint ligation, splint runs out of gel; (3) Hybridization to the blue complementary strand before and (4) after ligation. M = size marker (linear ds DNA). (**G**) PAGE analysis of the ligation experiment at 37 °C of all nicked circles $N_{bp} = 67 - 105\ bp$, that are distributed between 8 pools as annotated. Note that some circles split into two bands (73, 83, 93, and 103 bp) indicating different topoisomers of the same length. Band splitting indicates that those circles are a half-integer multiple of the equilibrium (torsionally relaxed) helical repeat $h_0$, or $N_{bp} \approx (n + \frac{1}{2})h_0$. Ligase concentration in the final ligation step (D to E) was 100-fold lower in experiment **H** (4 U/µl). Uncropped gel images, an independent repeat of experiment **G** and of a 0.1X [ligase] experiment are shown in **Fig. S3**.*

To find a potential change of $h_0$ upon bending, we circularized linear oligonucleotides with all lengths between 67-105 nucleotides (nt) with a 'splint' into single-stranded circles (**Fig. 2A**). Four to five oligonucleotides with a $\Delta N_{bp} = 4\ nt$ were pooled together into eight different subpools to fit all experiments on one gel and to allow for a better relative comparison between them as indicated in **Fig. 2G**. All strands share the same 13 nt sequences at the ends, such that one common 26 nt splint can be used for all strands. We used a similar pooling and circularization approach in a work describing the discovery of a template length-dependent amplification bias in rolling circle amplification (*28*). Single-stranded circles formed with near-quantitative yields, as most of the complex is single-stranded and therefore very flexible, entropically favoring circularization over dimerization (**Fig. 2B**). Addition of the complementary blue strands (**Fig. 2C**, linear) forms the respective nicked circles. The sequences in between the common splint-binding domains are unique such that each ss circle can only hybridize to the correct counterstrand. The resulting nicked circles (**Fig. 2D**) were then enzymatically ligated into

topologically closed double-stranded (ds) circles (**Fig. 2E**).The different species including linear strands, single- and double-stranded circles, can be separated by denaturing PAGE (polyacrylamide gel electrophoresis), (**F-H**), which also separates ss circles and linear strands.

The gels in **Fig. 2G-H** show the circular double-stranded region of ligation experiments at 37 °C at 1X ligase concentration (**G**) and a 100-fold lower [ligase] (**H**). Most $N_{bp}$ show only one band but the circles at $N_{bp}$ = 73, 83, 92/93 and 103 bp, split into two bands, which can be explained by the formation of two topoisomers with the same $N_{bp}$ (*5*).

**Equilibrium helical repeat is curvature-dependent**

From this gel data, we determined the equilibrium helical repeat $h_0$ (**Fig. 3A-B)**. Circles that were experimentally observed are highlighted blue, and those that should have been observed if $h_0$ was constant at $h_0$ =10.5 bp/turn are in red. In most experimental conditions, gel band intensities were similar which made it difficult to determine $h_0$ through the ligation efficiency maxima where $N_{bp} \approx nh_0$. Although stacking is a rare event for torsionally strained circles (**Fig. 1E**), ligations take several minutes and yields were still near-quantitative irrespective of $N_{bp}$. Even at reduced [ligase] (**Fig. 2H, Fig. S3**) or increased [salt] (**Fig. S6**), maxima remained too broad for an accurate determination of $h_0$. On the other hand, at those $N_{bp}$ where two topoisomers are observed, the torsional energy for unwinding (negative torque) or overwinding (positive torque) to match the ends (**Fig. 1C**, left) must be roughly equal, which is only the case if $N_{bp} \approx \left(n + \frac{1}{2}\right) h_0$. This condition is equivalent to a deviation from the torsionally relaxed twist $Tw_0 = N_{bp}/h_0$. At the band splitting, $\Delta Tw \approx \pm\frac{1}{2}$, where $\Delta Tw = Lk - Tw_0$ is the excess twist for a ligated circle with linking number $Lk$. For any other length, only the topoisomer with the least torsional stress (the lowest $\Delta Tw$) is observed (see **Supplementary Note 4**). We conclude that $N_{bp} = 73\ bp \approx 6.5\ h_0$ so $h_0 \approx 73\ bp\ /6.5\ turns\ \approx 11.2\ bp/turns$. Likewise, for $N_{bp} = 83$, $h_0 \approx 83\ bp\ /7.5\ turns\ \approx 11.1\ bp/turns$ and so on (**Fig. 3A**). If $h_0$ were constant at $h_0 = 10.5\ bp/turn$, two topoisomers should have been observed around $N_{bp} \approx 68, 79, 89,$ and $100\ bp$ (red vertical lines). In **Fig. 3B**, the sum of the twist and bend deformation energy, $E_{\mathrm{circ}} = E_{\mathrm{Tw}} + E_{\mathrm{bend}}$, is plotted (**Supplementary Note 4**). Circles are torsionally relaxed if they lie on the observed $h_0$ curve in **Fig. 3A**, which connects the helical repeats at the local minima of the energy shown in **Fig. 3B**. In summary, our data proves that $h_0$ is curvature-dependent and that DNA unwinds when tightly bent (see also **Fig. 5**).

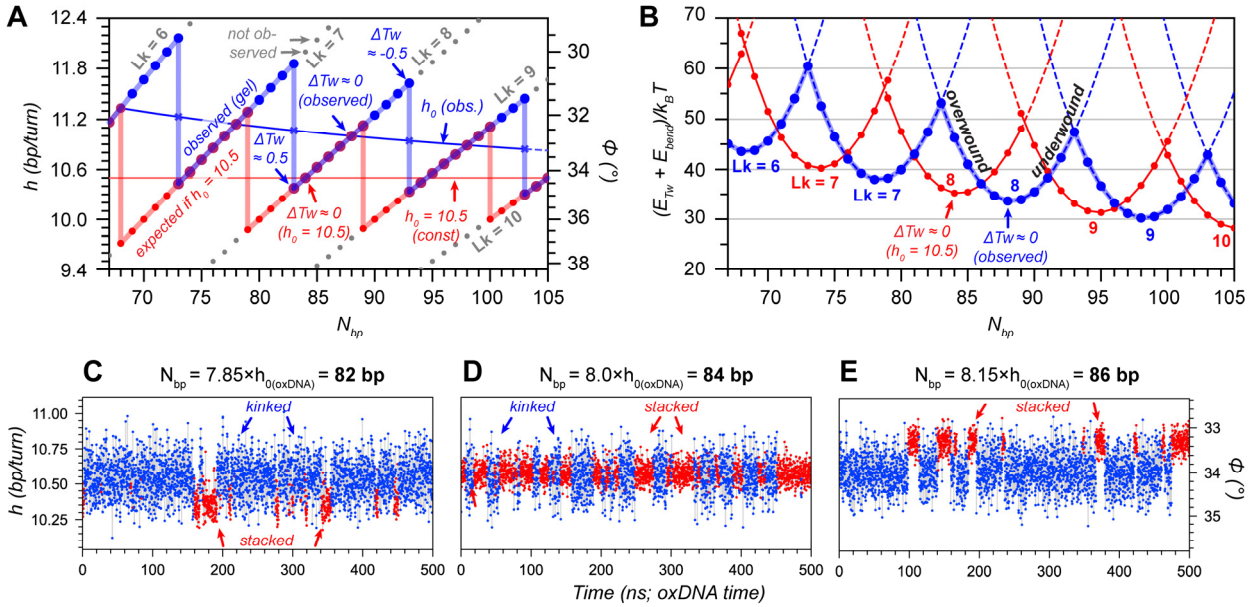


***Fig. 3: Twist-bend coupling (TBC, A), energy landscapes (B) and kymographs of stacking (C-E).*** *(**A**) The helical repeat $h = N_{bp} / Lk$ for theoretically possible and experimentally observed ligated circles. **Blue**: Experimentally observed circles (**Fig. 2**). Vertical lines indicate $N_{bp}$ where two topoisomers were found. **Red** datapoints: circles that should have been observed for a constant $h_0 = 10.5\ bp/turn$. Circles with $h = h_0$ are torsionally relaxed ($\Delta Tw = 0$), $h > h_0$ are underwound ($\Delta Tw < 0$), and $h < h_0$ are overwound ($\Delta Tw > 0$). Where two topoisomers are observed, $h_0 \approx N_{bp} / \left(n \pm \frac{1}{2}\right)$ or $\Delta Tw \approx \pm\frac{1}{2}$ (**Supplementary Note 4**). (**B**) The total mechanical energy in stacked or ligated circles is the sum of twisting energy $E_{Tw}$ and bending energy $E_{bend}$. At the local minima, circles are torsionally relaxed; to the left they are overwound, to the right underwound. Red: theoretical energy landscape if $h_0 = 10.5\ bp/turns$ was constant and independent of curvature. (**C-E**) Analysis of $h$ in oxDNA simulations of 82 (C), 84 (D) and 86 bp nicked circles (E), where $h = 360°/\phi$ (scale on left) was calculated from the average twist angle $\phi$ between adjacent base pairs (scale on right). The outermost 2 bp can fray and were excluded from analysis. Stacked conformations (red) and kinked conformations (blue) have ns lifetimes (in ox-DNA timescale). Note that for all three circles, the kinked conformations fluctuate around the equilibrium $h_0$ of oxDNA (10.55 bp/turn), while stacked conformations can be overwound (C) or underwound (E).*

### [Ligase] does not influence helical repeat

Lifetimes of both looped and linear configurations in classical circularization experiments (**Fig. 1A**) can be on the order of seconds or minutes (*10*, *15*) and ligations in these experiments must be performed at very low ligase concentrations to avoid shifting the equilibria (*11*). On the other hand, transitions between stacked and kinked configurations in our essay are much more dynamic with lifetimes on the order of nanoseconds (**Fig. 3C-E**, **Fig. S5**). Note that coarse-graining results in an increased diffusion coefficient in oxDNA so that simulated time scales are

10-100 times shorter than those in experiment (29, 26). As ligation experiments take minutes to complete, we hypothesized that the concentration of the ligase will not influence equilibria as it does in classical looping experiments. Indeed, we found that decreasing the ligase concentration by 1-2 orders of magnitude (**Fig. 2H, Fig. S3**) decreased the overall intensity of bands around $\Delta Tw = \pm\frac{1}{2}$ and most ss circles do not ligate into ds circles (87-105 nt on bottom right). Band splitting is still visible at the same lengths as for high ligase concentration (**Fig. 2G**), from which we conclude that the helical repeat is not significantly changed by [ligase]. On the other hand, DNA unwinds at high temperatures and low salinity (*18*, *30*), and both trends are captured by oxDNA simulations and ligation experiments (**Fig. S6**) (**Fig. S7**).

### All-Atom MD simulations

We next explored the conformational stability of selected nicked and ligated circles under varying torsional strain through all atom MD simulations (**Fig. 4**). Previous studies (*21–23*) suggested that ligated circles with $N_{bp} = 90\ bp$ and $Lk = 8$ are torsionally relaxed, so $h_0 \approx 11.25\ bp/turn$ - about the same as $h_0$ for linear DNA in that model . We found that circles with $\Delta Tw \approx 0$ remained stacked for at least 50 ns even when nicked (**A**, **D**), whereas nicked circles with a $\Delta Tw \approx \pm\frac{1}{2}$ (**B, C**) kinked within 5 ns. Nicked circles with $\Delta Tw \approx 1$ (**G-H**) kinked within few 100 ps and resolved the $\Delta Tw$ to around zero. Re-stacking was not observed on this timescale. Ligated circles with $\Delta Tw = \pm\frac{1}{2}$ (**E-F**) were stable for the entire simulation without kinking or significant writhe, indicating that circles where topoisomer splitting was observed after ligation in the experiments (**Fig. 3G**) are also structurally stable.

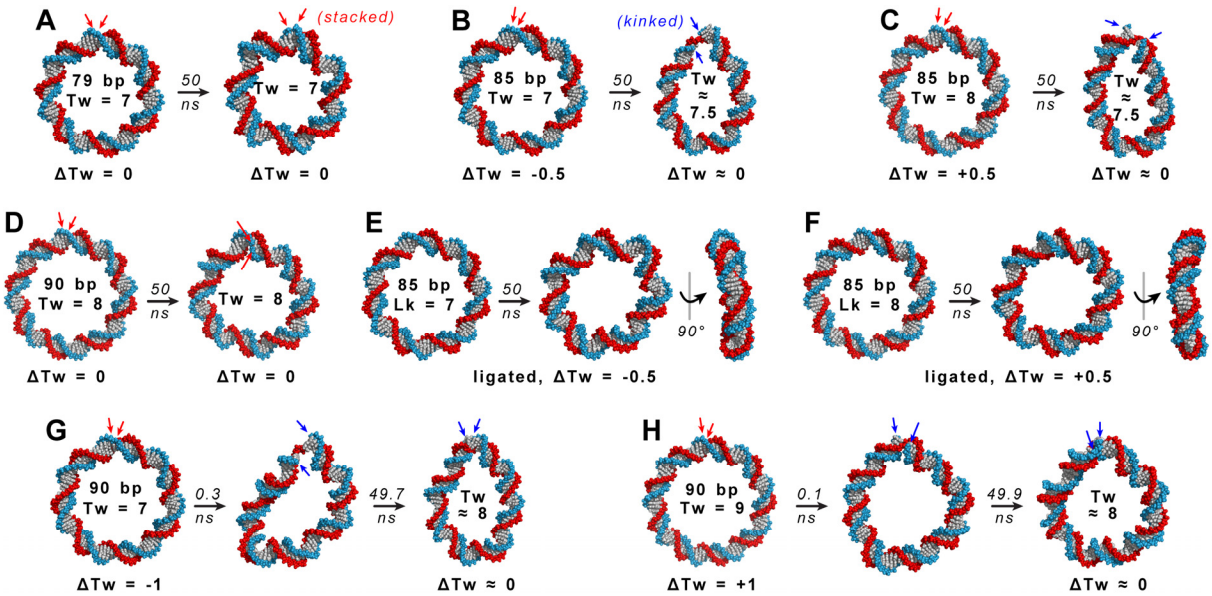


***Fig. 4. All-atom MD simulations.*** *Several nicked (**A-D, G-H**) and ligated (**E-F**) circles with varying $\Delta Tw$ were simulated for 50 ns; movies of all trajectories can be found in the supporting information. **Red arrows** indicate stacked ends, **blue arrows** unstacked. Discussion see text.*

## Discussion

DNA's structural properties are often probed experimentally by stretching and twisting DNA and measuring the response. For example, the force-extension curves at low forces measured through pulling experiments of entropically coiled DNA allow one to determine the persistence length (*31*). Twist, bend, and stretch deformations in DNA are coupled. Twist-stretch coupling was found with magnetic torque tweezers (MTT) (*32*, *33*) where DNA counterintuitively slightly overwinds at small forces (<20-30 pN) and unwinds at higher forces. Tension in our minicircles is only ~3-5 pN (see **Fig. S8** and Supplementary Note 5), and the influence of twist-stretch coupling on the helical repeat is therefore negligible.

TBC was theoretically introduced decades ago by MS (*17*) who predicted that tight bending unwinds DNA. This is not detectable by classical looping assys (**Fig. 1A-B, Fig. 5**) due to the small synthesis yields or the release of torsional stress through kinking and twisting. Some evidence for TBC is seen in MTT experiments with long, supercoiled DNA, where MS's model better describes the force dependence of the effective torsional stiffness than the TWLC model (*34*). A direct quantification $h_0$ as in our experiments would, however, be difficult with MTT experiments as these require fragments where $L \gg l_p$ and cannot produce defined tight curvatures in a controllable way.

Recent TBC estimates from MD simulations and MTT data (*35*, *36*) predict a widening of $h_0$ by only 0.2 % at the curvature of the nucleosome (**Fig. 5**, red curve; see Suppl. Note 4), which should be experimentally indetectable. Our data and the magnitude of the relative difference in helical repeat (~10 %), however, is in almost perfect agreement with the predictions from the original MS paper, which explained the small unwinding suggested from the data available of the time (**Fig. 5**, black datapoints (*5–7*)). While Eq. 31 is an excellent fit to the helical repeat data, the value of the TBC parameters may indicate that additional physics is at play. General stability requirements of the MS model are difficult to satisfy when the twist-bend coupling parameter exceeds the torsional stiffness (see Suppl. Note 4). TBC parameter estimates from ref. (*35*, *36*) satisfy the stability constraints naturally, but dramatically underestimate the magnitude of the widening of $h_0$.

One possibility outside this model is the influence of the ligase on the helical repeat. However, a local maximum in Vafabakhsh's ligase-free looping experiments occurred around 99 bp (and not 94-95) consistent with a larger helical repeat (see Fig. 3E in ref. (*10*)). Moreover, reducing the ligase concentration 100-fold (**Fig. 2H**) did not influence the helical repeat.

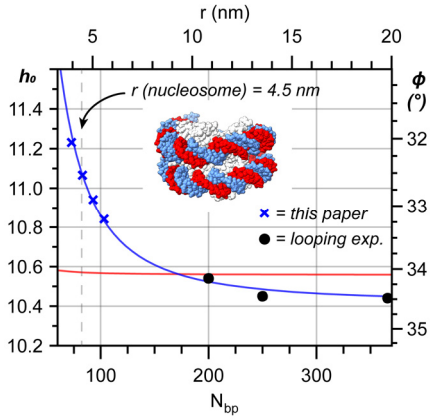


***Fig. 5. Extent of TBC.*** *Relaxed helical repeat of a duplex bent with a constant radius of curvature $r$ (top axis) matching that of a minicircle of $N_{bp}$ base pairs (bottom axis). Blue, experimental datapoints from this study, black datapoints from classical circularization experiments (5–7). Fit using the Marko/Siggia model (17) to both data sets give a relaxed helical repeat of $h_{(\kappa=0)} = 10.42\ bp/turn$ (=linear DNA) and TBC parameter ($G/C$ = 2.7), where $G$ is the twist bend coupling parameter and $C$ is the torsional stiffness. Red curve, TBC prediction with parameters from ref. (35, 36).*

In biology, DNA is often tightly bent. For example, ~72% of eukaryotic DNA is nucleosomal DNA. Our experiments show a widening of the $h_0$ by ~6 % if DNA is bent to the same curvature as in nucleosomes. A $\Delta Tw$ of ~1.2 turns per nucleosome results in a twist energy of $E_{Tw} \approx 60\ k_BT \approx 35.4\ kcal/mol$ (eq. 13) in addition to a bending stress $E_{bend} \approx 60\ k_BT$ (eq. 15). The total mechanical stress in a nucleosome is therefore $E_{Tw} + E_{bend} \approx 120\ k_B$T, which must be compensated through noncovalent interactions between the DNA and histone proteins. The increase of $h_0$ and aggravates the linking number paradox (36) and the additional torsional stress likely influences DNA wrapping and unwrapping dynamics (37) that is necessary for gene regulation and expression. DNA is also highly compacted in virus capsids with a radius of curvature as low as 3 nm (*2*) while the mechanism of packing may be influenced by twisting (*37*). Next, transcription factors that loop DNA such as the *lac* repressor play important roles in the regulation of genes in prokaryotes an eukaryotes and can have radii of curvatures of less than 5 nm (*2*). A helical repeat of 11-11.3 bp/turn was determined for the loops between the two binding sites of the lac repressor (*38*), araCBAD (*39*) and HU protein induced loops (*40*), consistent with TBC and our data.

Next, the curvature-dependence of the helical repeat will also have to be considered in the design of DNA nanostructures that contain small minicircles such as DNA catenanes (*41*), rotaxanes (*42*), DNA-encircled lipid nanodiscs (*43*), or for tightly bent DNA origami structures (*44*, *45*). Physical models of DNA need to be corrected for tightly bent DNA. Finally, TBC acts in both directions and just as torque from MTT induces bending (*34*), so will torque from helicases, polymerases or DNA packing motors. We conclude that TBC likely plays a role in all processes where DNA is tightly bent or twisted.

## References and Notes


1. A. Basu, D. G. Bobrovnikov, T. Ha, DNA mechanics and its biological impact. *J. Mol. Biol.* **433**, 166861 (2021).

2. H. G. Garcia, P. Grayson, L. Han, M. Inamdar, J. Kondev, P. C. Nelson, R. Phillips, J. Widom, P. A. Wiggins, Biological consequences of tightly bent DNA: The other life of a macromolecular celebrity. *Biopolymers* **85**, 115–130 (2007).

3. J. Shimada, H. Yamakawa, Ring-closure probabilities for twisted wormlike chains. Application to DNA. *Macromolecules* **17**, 689–698 (1984).

4. D. Shore, J. Langowski, R. L. Baldwin, DNA flexibility studied by covalent closure of short fragments into circles. *Proc. Natl. Acad. Sci.* **78**, 4833–4837 (1981).

5. D. Shore, R. L. Baldwin, Energetics of DNA twisting: II. Topoisomer analysis. *J. Mol. Biol.* **170**, 983–1007 (1983).

6. D. S. Horowitz, J. C. Wang, Torsional rigidity of DNA and length dependence of the free energy of DNA supercoiling. *J. Mol. Biol.* **173**, 75–91 (1984).

7. W. H. Taylor, P. J. Hagerman, Application of the method of phage T4 DNA ligase-catalyzed ring-closure to the study of DNA structure: II. NaCl-dependence of DNA flexibility and helical repeat. *J. Mol. Biol.* **212**, 363–376 (1990).

8. A. J. Spakowitz, Wormlike chain statistics with twist and fixed ends. *Europhys. Lett.* **73**, 684 (2006).

9. T. E. Cloutier, J. Widom, Spontaneous Sharp Bending of Double-Stranded DNA. *Mol. Cell* **14**, 355–362 (2004).

10. R. Vafabakhsh, T. Ha, Extreme Bendability of DNA Less than 100 Base Pairs Long Revealed by Single-Molecule Cyclization. *Science* **337**, 1097–1101 (2012).

11. Q. Du, C. Smith, N. Shiffeldrim, M. Vologodskaia, A. Vologodskii, Cyclization of short DNA fragments and bending fluctuations of the double helix. *Proc. Natl. Acad. Sci.* **102**, 5397–5402 (2005).

12. A. Vologodskii, Q. Du, M. D. Frank-Kamenetskii, Bending of short DNA helices. *Artif. DNA PNA XNA* **4**, 1–3 (2013).

13. A. Vologodskii, M. D. Frank-Kamenetskii, Strong bending of the DNA double helix. *Nucleic Acids Res.* **41**, 6785–6792 (2013).

14. R. M. Harrison, F. Romano, T. E. Ouldridge, A. A. Louis, J. P. K. Doye, Identifying Physical Causes of Apparent Enhanced Cyclization of Short DNA Molecules with a Coarse-Grained Model. *J. Chem. Theory Comput.* **15**, 4660–4672 (2019).

15. T. T. Le, H. D. Kim, Probing the elastic limit of DNA bending. *Nucleic Acids Res.* **42**, 10786–10794 (2014).

16. J. Jeong, H. D. Kim, Determinants of cyclization–decyclization kinetics of short DNA with sticky ends. *Nucleic Acids Res.* **48**, 5147–5156 (2020).

17. J. F. Marko, E. D. Siggia, Bending and twisting elasticity of DNA. *Macromolecules* **27**, 981–988 (1994).

18. J. C. Wang, Helical repeat of DNA in solution. *Proc. Natl. Acad. Sci.* **76**, 200–203 (1979).

19. J. J. Hayes, T. D. Tullius, A. P. Wolffe, The structure of DNA in a nucleosome. *Proc. Natl. Acad. Sci.* **87**, 7405–7409 (1990).

20. D. Vasudevan, E. Y. D. Chua, C. A. Davey, Crystal Structures of Nucleosome Core Particles Containing the '601' Strong Positioning Sequence. *J. Mol. Biol.* **403**, 1–10 (2010).

21. J. Yoo, S. Park, C. Maffeo, T. Ha, A. Aksimentiev, DNA sequence and methylation prescribe the inside-out conformational dynamics and bending energetics of DNA minicircles. *Nucleic Acids Res.* **49**, 11459–11475 (2021).

22. M. Kim, S. Bae, I. Oh, J. Yoo, J. S. Kim, Sequence-dependent twist-bend coupling in DNA minicircles. *Nanoscale* **13**, 20186–20196 (2021).

23. M. Kim, C. C. Hong, S. Lee, J. S. Kim, Dynamics of a DNA minicircle: Poloidal rotation and in-plane circular vibration. *Bull. Korean Chem. Soc.* **43**, 523–528 (2022).

24. E. Poppleton, J. Bohlin, M. Matthies, S. Sharma, F. Zhang, P. Šulc, Design, optimization and analysis of large DNA and RNA nanostructures through interactive visualization, editing and molecular simulation. *Nucleic Acids Res.* **48**, e72 (2020).

25. J. Bohlin, M. Matthies, E. Poppleton, J. Procyk, A. Mallya, H. Yan, P. Šulc, Design and simulation of DNA, RNA and hybrid protein–nucleic acid nanostructures with oxView. *Nat. Protoc.* **17**, 1762–1788 (2022).

26. A. Sengar, T. E. Ouldridge, O. Henrich, L. Rovigatti, P. Sulc, A primer on the oxDNA model of DNA: When to use it, how to simulate it and how to interpret the results. *Front. Mol. Biosci.* **8**, 693710 (2021).

27. S. K. Nomidis, M. Caraglio, M. Laleman, K. Phillips, E. Skoruppa, E. Carlon, Twist-bend coupling, twist waves, and the shape of DNA loops. *Phys. Rev. E* **100**, 022402 (2019).

28. B. Joffroy, Y. O. Uca, D. Prešern, J. P. K. Doye, T. L. Schmidt, Rolling circle amplification shows a sinusoidal template length-dependent amplification bias. *Nucleic Acids Res.* **46**, 538–545 (2018).

29. B. E. K. Snodin, F. Romano, L. Rovigatti, T. E. Ouldridge, A. A. Louis, J. P. K. Doye, Direct Simulation of the Self-Assembly of a Small DNA Origami. *ACS Nano* **10**, 1724–1737 (2016).

30. F. Kriegel, C. Matek, T. Dršata, K. Kulenkampff, S. Tschirpke, M. Zacharias, F. Lankaš, J. Lipfert, The temperature dependence of the helical twist of DNA. *Nucleic Acids Res.* **46**, 7998–8009 (2018).

31. C. Bustamante, J. F. Marko, E. D. Siggia, S. Smith, Entropic Elasticity of λ-Phage DNA. *Science* **265**, 1599–1600 (1994).

32. T. R. Strick, J.-F. Allemand, D. Bensimon, A. Bensimon, V. Croquette, The Elasticity of a Single Supercoiled DNA Molecule. *Science* **271**, 1835–1837 (1996).

33. J. Gore, Z. Bryant, M. Nöllmann, M. U. Le, N. R. Cozzarelli, C. Bustamante, DNA overwinds when stretched. *Nature* **442**, 836–839 (2006).

34. S. K. Nomidis, F. Kriegel, W. Vanderlinden, J. Lipfert, E. Carlon, Twist-Bend Coupling and the Torsional Response of Double-Stranded DNA. *Phys. Rev. Lett.* **118**, 217801 (2017).

35. E. Skoruppa, M. Laleman, S. K. Nomidis, E. Carlon, DNA elasticity from coarse-grained simulations: The effect of groove asymmetry. *J. Chem. Phys.* **146**, 214902 (2017).

36. S. K. Nomidis, E. Skoruppa, E. Carlon, J. F. Marko, Twist-bend coupling and the statistical mechanics of the twistable wormlike-chain model of DNA: Perturbation theory and beyond. *Phys. Rev. E* **99**, 032414 (2019).

37. A. J. Spakowitz, Z.-G. Wang, DNA Packaging in Bacteriophage: Is Twist Important? *Biophys. J.* **88**, 3912–3923 (2005).

38. J. Müller, S. Oehler, B. Müller-Hill, Repression oflacPromoter as a Function of Distance, Phase and Quality of an AuxiliarylacOperator. *J. Mol. Biol.* **257**, 21–29 (1996).

39. T. L. Schmidt, A. Heckel, Construction of a Structurally Defined Double-Stranded DNA Catenane. *Nano Lett.* **11**, 1739–1742 (2011).

40. D. Ackermann, T. L. Schmidt, J. S. Hannam, C. S. Purohit, A. Heckel, M. Famulok, A double-stranded DNA rotaxane. *Nat Nanotechnol* **5**, 436–442 (2010).

41. K. Iric, M. Subramanian, J. Oertel, N. P. Agarwal, M. Matthies, X. Periole, T. P. Sakmar, T. Huber, K. Fahmy, T. L. Schmidt, DNA-encircled lipid bilayers. *Nanoscale* **10**, 18463–18467 (2018).

42. H. Dietz, S. M. Douglas, W. M. Shih, Folding DNA into Twisted and Curved Nanoscale Shapes. *Science* **325**, 725–730 (2009).

43. D. Han, S. Pal, J. Nangreave, Z. Deng, Y. Liu, H. Yan, DNA Origami with Complex Curvatures in Three-Dimensional Space. *Science* **332**, 342–346 (2011).

44. J. Schindelin, I. Arganda-Carreras, E. Frise, V. Kaynig, M. Longair, T. Pietzsch, S. Preibisch, C. Rueden, S. Saalfeld, B. Schmid, J.-Y. Tinevez, D. J. White, V. Hartenstein, K. Eliceiri, P. Tomancak, A. Cardona, Fiji: an open-source platform for biological-image analysis. *Nat. Methods* **9**, 676–682 (2012).

45. J. Walther, M. Orozco, *MC_DNA: A Web Server for the Detailed Study of the Structure and Dynamics of DNA and Chromatin Fibers* (https://mmb.irbbarcelona.org/MCDNA/).

46. A. Pérez, I. Marchán, D. Svozil, J. Sponer, T. E. Cheatham, C. A. Laughton, M. Orozco, Refinement of the AMBER force field for nucleic acids: improving the description of α/γ conformers. *Biophys. J.* **92**, 3817–3829 (2007).

47. W. D. Cornell, P. Cieplak, C. I. Bayly, I. R. Gould, K. M. Merz, D. M. Ferguson, D. C. Spellmeyer, T. Fox, J. W. Caldwell, P. A. Kollman, A second generation force field for the simulation of proteins, nucleic acids, and organic molecules. *J. Am. Chem. Soc.* **117**, 5179–5197 (1995).

48. J. Yoo, A. Aksimentiev, Improved parameterization of amine–carboxylate and amine–phosphate interactions for molecular dynamics simulations using the CHARMM and AMBER force fields. *J. Chem. Theory Comput.* **12**, 430–443 (2016).

49. J. Yoo, A. Aksimentiev, New tricks for old dogs: improving the accuracy of biomolecular force fields by pair-specific corrections to non-bonded interactions. *Phys. Chem. Chem. Phys.* **20**, 8432–8449 (2018).

50. B. Hess, H. Bekker, H. J. Berendsen, J. G. Fraaije, LINCS: A linear constraint solver for molecular simulations. *J. Comput. Chem.* **18**, 1463–1472 (1997).

51. T. Darden, D. York, L. Pedersen, Particle mesh Ewald: An N· log (N) method for Ewald sums in large systems. *J. Chem. Phys.* **98**, 10089–10092 (1993).

52. G. Bussi, D. Donadio, M. Parrinello, Canonical sampling through velocity rescaling. *J. Chem. Phys.* **126** (2007).

53. M. Parrinello, A. Rahman, Polymorphic transitions in single crystals: A new molecular dynamics method. *J. Appl. Phys.* **52**, 7182–7190 (1981).

54. W. Humphrey, A. Dalke, K. Schulten, VMD: visual molecular dynamics. *J. Mol. Graph.* **14**, 33–38 (1996).

55. H. Jacobson, W. H. Stockmayer, Intramolecular Reaction in Polycondensations. I. The Theory of Linear Systems. *J. Chem. Phys.* **18**, 1600–1606 (1950).

56. A. Basu, D. G. Bobrovnikov, Z. Qureshi, T. Kayikcioglu, T. T. M. Ngo, A. Ranjan, S. Eustermann, B. Cieza, M. T. Morgan, M. Hejna, H. T. Rube, K.-P. Hopfner, C. Wolberger, J. S. Song, T. Ha, Measuring DNA mechanics on the genome scale. *Nature* **589**, 462–467 (2021).

57. A. D. Bates, A. Maxwell, DNA gyrase can supercoil DNA circles as small as 174 base pairs. *EMBO J.* **8**, 1861–1866 (1989).

58. Q. Du, A. Kotlyar, A. Vologodskii, Kinking the double helix by bending deformation. *Nucleic Acids Res* **36**, 1120 (2008).

59. X. Gao, Y. Hong, F. Ye, J. T. Inman, M. D. Wang, Torsional Stiffness of Extended and Plectonemic DNA. *Phys. Rev. Lett.* **127**, 028101 (2021).

60. J. Lipfert, J. W. J. Kerssemakers, T. Jager, N. H. Dekker, Magnetic torque tweezers: measuring torsional stiffness in DNA and RecA-DNA filaments. *Nat. Methods* **7**, 977–980 (2010).

**Acknowledgments:** We thank Dr. Michael Matthies, Dr. Petr Sulc, Dr. Christopher Maffeo and Dr. Aleksei Aksimentiev for helpful discussions.

**Funding:**

This research was supported by the National Institutes of Health, National Institute of General Medical Sciences through MIRA grant #R35GM142706 to TLS, and the National Science Foundation through an EAGER grant #2117998 to TLS.

**Author contributions:**

Conceptualization: TLS, JP

Experiments: SC, DH

oxDNA simulations and analysis: DRH, TS, RB

All-atom MD simulations: FF

Data analysis and visualization: all authors

Funding acquisition: TLS

Supervision: TLS, JP

Writing – original draft: TLS

Writing – review & editing: all authors

**Competing interests:** Authors declare that they have no competing interests.

**Data and materials availability:** Code written for this study is available at https://github.com/tls-dna/twist-bend_public. Raw experimental or simulation data is available upon request.

**Supplementary Materials**

Materials and Methods

Supplementary Text

Figs. S1 to S#11

Table S1

Movies S1 to S#